

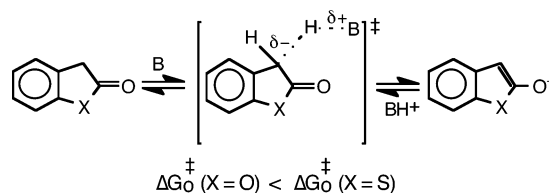
Kinetics of Proton Transfer from Benzo[*b*]-2,3-dihydrofuran-2-one and Benzo[*b*]-2,3-dihydrothiophene-2-one. Effect of Anion Aromaticity on Intrinsic Barriers

Claude F. Bernasconi* and Huaiben Zheng

Department of Chemistry and Biochemistry, University of California, Santa Cruz, California 95064

bernasconi@chemistry.ucsc.edu

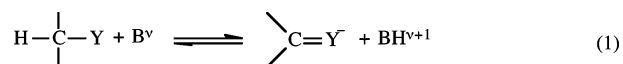
Received July 31, 2006



Rates of the reversible deprotonation of benzo[*b*]-2,3-dihydrofuran-2-one (**6H-O**) and benzo[*b*]-2,3-dihydrothiophene-2-one (**6H-S**) by OH^- , primary aliphatic amines, secondary alicyclic amines, and carboxylate ions have been determined in water at 25 °C. As noted earlier by Kresge and Meng, **6H-S** ($\text{p}K_a = 8.82$) is considerably more acidic than **6H-O** ($\text{p}K_a = 11.68$), which mainly reflects the greater aromatic stabilization of the conjugate base of **6H-S** (thiophene derivative) compared to that of **6H-O** (furan derivative). The main focus of this paper is to assess how the difference in the aromaticity of the two enolate ions affects the intrinsic barrier to the proton transfer. These intrinsic barriers were determined from Brønsted plots for the reactions with the amines and carboxylate ions or calculated on the basis of the Marcus equation for the reactions with OH^- . They are consistently somewhat higher for the reactions of **6H-S** than for the reactions of **6H-O**, implying that the aromaticity in the anion enhances the intrinsic barrier. This contrasts with a previous report on the deprotonation of some cyclic rhenium Fischer-type carbene complexes where the reaction that leads to the most aromatic conjugate base (thiophene derivative) has a *lower* intrinsic barrier than the reaction that leads to the less aromatic furan analogue. We are offering a detailed analysis of other potential factors that may affect the intrinsic barriers and which could explain these contradictory results.

Introduction

It is now well established¹ that reactions that convert resonance-stabilized/-delocalized reactants into products that lack such stabilization, or reactions that convert nondelocalized reactants into products that enjoy such delocalization/resonance stabilization, have relatively high intrinsic barriers (ΔG_0^\ddagger) or low intrinsic rate constants (k_0).² This feature is particularly well documented for proton transfers from carbon acids that are activated by π -acceptors (eq 1), and there is good agreement



between experimental results^{1,5–8} and computational/theoretical studies.^{9–14} Examples from other reaction families have also been reported such as nucleophilic additions to alkenes or vinylic

(3) Marcus, R. A. *J. Phys. Chem.* **1968**, *72*, 891.

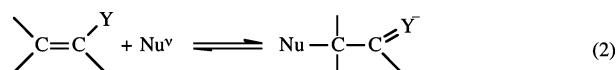
(4) Keeffe, J. R.; Kresge, A. J. In *Investigation of Rates and Mechanisms of Reactions*; Bernasconi, C. F., Ed.; Wiley-Interscience: New York, 1986; Part 1, p 747.

(5) (a) Bernasconi, C. F.; Sun, W.; García-Río, L.; Kin-Yan; Kittredge, K. *J. Am. Chem. Soc.* **1997**, *119*, 5583. (b) Bernasconi, C. F.; Ali, M. *J. Am. Chem. Soc.* **1999**, *121*, 3039. (c) Bernasconi, C. F.; Sun, W. *J. Am. Chem. Soc.* **2002**, *124*, 2799. (d) Bernasconi, C. F.; Ali, M.; Gunter, J. C. *J. Am. Chem. Soc.* **2003**, *125*, 151. (e) Bernasconi, C. F.; Fairchild, D. E.; Montañez, R. L.; Aleshi, P.; Zheng, H.; Lorance, E. *J. Org. Chem.* **2005**, *70*, 7721. (f) Bernasconi, C. F.; Ragains, M. L. *J. Organomet. Chem.* **2005**, *690*, 5616.

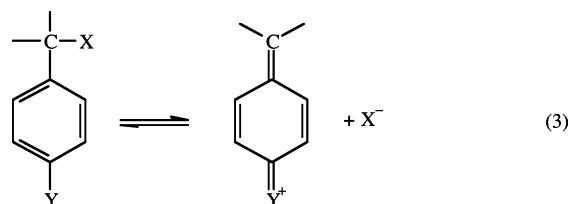
(1) (a) Bernasconi, C. F. *Acc. Chem. Res.* **1987**, *20*, 301. (b) Bernasconi, C. F. *Acc. Chem. Res.* **1992**, *25*, 9. (c) Bernasconi, C. F. *Adv. Phys. Org. Chem.* **1992**, *27*, 119. (d) Bernasconi, C. F. *Chem. Soc. Rev.* **1997**, *26*, 299. (e) Bernasconi, C. F. *Adv. Phys. Org. Chem.* **2002**, *37*, 13.

(2) The intrinsic barrier (intrinsic rate constant) of a reaction with a forward rate constant k_1 and a reverse rate constant k_{-1} is defined as $\Delta G_1^\ddagger = \Delta G_{-1}^\ddagger = \Delta G^\ddagger$ when $\Delta G^\circ = 0$ (as $k_0 = k_1 = k_{-1}$ when $K_1 = 1$).^{3,4}

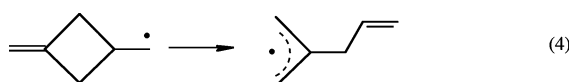
compounds activated by π -acceptors^{1,15} (eq 2), the formation



of carbocations stabilized by π -donors,^{1c,16} for example, eq 3,

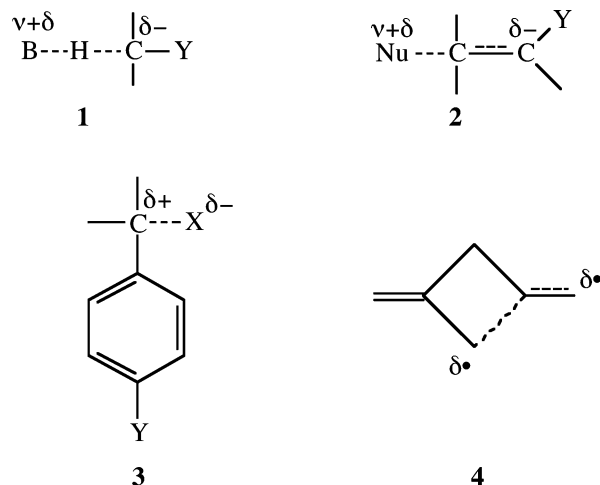


and the formation of delocalized radicals,^{1c,17} for example, eq 4.



The underlying reason for the high intrinsic barriers appears to be the same irrespective of the type of reaction: the transition state is imbalanced in the sense that delocalization lags behind bond changes when the reaction leads to delocalized products, while the loss of delocalization runs ahead of bond changes in reactions of delocalized reactants.^{1a-1c} Structures **1**–**4** are schematic and somewhat exaggerated representations of the imbalanced transition states of reactions 1–4, respectively.

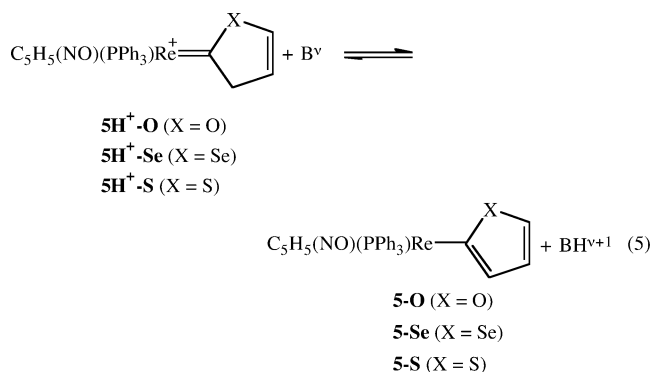
Because of the lag in charge delocalization, the transition state derives only a minimal benefit from the stabilizing effect of



the product resonance, and this is the reason the intrinsic barrier is high. The same barrier enhancement occurs in the reverse direction because most of the product stabilization due to delocalization is being lost at the transition state. Hence, the greater the degree of resonance stabilization in the reactant or product, the higher the intrinsic barrier.

This relationship between intrinsic barriers and transition-state imbalances is the manifestation of a more general principle called the principle of nonperfect synchronization (PNS).^{1a-c} It states that when a product-stabilizing feature lags behind bond changes at the transition state the intrinsic barrier increases while the intrinsic barrier decreases if the product-stabilizing feature is more advanced at the transition state than bond changes. This is a principle that is mathematically provable and can have no exceptions.^{1c}

In a recent study of proton transfers from rhenium Fischer-type carbene complexes,¹⁸ eq 5, we addressed the question of whether reactions that lead to the formation of an aromatic product follow the same rules as the reactions that lead to the formation of products stabilized by simple resonance. The



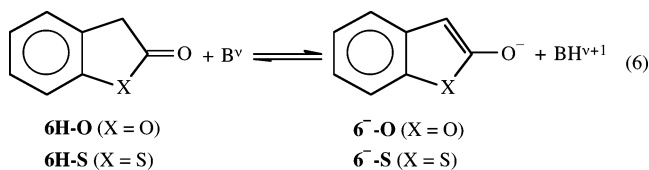
conjugate bases of these carbene complexes represent aromatic heterocycles, i.e., substituted furan (**5-O**), selenophene (**5-Se**), and thiophene (**5-S**) derivatives, respectively. The aromatic stabilization of these heterocycles is known to follow the order furan < selenophene < thiophene.¹⁹⁻²¹ As one would anticipate,

- (10) (a) Terrier, F.; Lelièvre, J.; Chatrousse, A.-P.; Farrell, P. *J. Chem. Soc., Perkin Trans. 2* **1985**, 1479. (b) Terrier, F.; Xie, H.-Q.; Lelièvre, J.; Boubaker, T.; Farrell, P. G. *J. Chem. Soc., Perkin Trans. 2* **1990**, 1899. (c) Moutiers, G.; El Fahid, B.; Collet, A.-G.; Terrier, F. *J. Chem. Soc., Perkin Trans. 2* **1996**, 49. (d) Moutiers, G.; El Fahid, B.; Goumont, R.; Chatrousse, A.-P.; Terrier, F. *J. Org. Chem.* **1996**, *61*, 1978.
- (11) (a) Nevy, J. B.; Hawkinson, D. C.; Blotny, G.; Yao, X.; Pollack, R. M. *J. Am. Chem. Soc.* **1997**, *119*, 12722. (b) Yao, X.; Gold, M. A.; Pollack, R. M. *J. Am. Chem. Soc.* **1999**, *121*, 6220.
- (12) Zhong, Z.; Snowden, T. S.; Best, M. D.; Anslyn, E. V. *J. Am. Chem. Soc.* **2004**, *126*, 3488.
- (13) Bekšic, D.; Bertrán, J.; Lluck, J. M.; Hynes, J. T. *J. Phys. Chem. A* **1998**, *102*, 3977.
- (14) (a) Saunders, W. H., Jr. *J. Am. Chem. Soc.* **1994**, *116*, 5400. (b) Saunders, W. H., Jr.; Van Verth, J. E. *J. Org. Chem. Soc.* **1994**, *60*, 3452. (c) Van Verth, J. E.; Saunders, W. H., Jr. *J. Org. Chem.* **1997**, *62*, 5743. (d) Van Verth, J. E.; Saunders, W. H., Jr. *Can. J. Chem.* **1999**, *77*, 810. (e) Harris, N.; Wei, W.; Saunders, W. H., Jr.; Shaik, S. S. *J. Phys. Org. Chem.* **1999**, *12*, 259. (f) Harris, N.; Wei, W.; Saunders, W. H., Jr.; Shaik, S. J. *Am. Chem. Soc.* **2000**, *112*, 6754.
- (15) (a) Bernasconi, C. F.; Wenzel, P. J. *J. Am. Chem. Soc.* **1994**, *116*, 5405. (b) Bernasconi, C. F.; Wenzel, P. J. *J. Am. Chem. Soc.* **1996**, *118*, 10494. (c) Bernasconi, C. F.; Wenzel, P. J.; Keeffe, J. R.; Gronert, S. *J. Am. Chem. Soc.* **1997**, *119*, 4008. (d) Bernasconi, C. F.; Wenzel, P. J. *J. Org. Chem.* **2001**, *66*, 968. (e) Bernasconi, C. F.; Wenzel, P. J. *J. Am. Chem. Soc.* **2001**, *123*, 7146. (f) Bernasconi, C. F.; Wenzel, P. J. *J. Org. Chem.* **2003**, *68*, 6870.
- (16) Yamataka, H.; Mustanir; Mishima, M. *J. Am. Chem. Soc.* **1999**, *121*, 10233.
- (17) Lee, I.; Kim, C. K. *J. Phys. Org. Chem.* **1999**, *12*, 255.
- (18) Costentin, C.; Savéant, J.-M. *J. Am. Chem. Soc.* **2004**, *126*, 14787.
- (19) (a) Bernasconi, C. F. *Tetrahedron* **1989**, *45*, 4017. (b) Bernasconi, C. F.; Ketner, R. J.; Ragains, M. L.; Chen, X.; Rappoport, Z. *J. Am. Chem. Soc.* **2001**, *123*, 2155. (c) Bernasconi, C. F.; Ketner, R. J.; Chen, X.; Rappoport, Z. *ARKIVOC* **2002** (xii), 161.
- (20) (a) Richard, J. P. *J. Am. Chem. Soc.* **1989**, *111*, 1455. (b) Richard, J. P. *J. Org. Chem.* **1994**, *59*, 25. (c) Richard, J. P.; Amyes, T. L.; Toteva, M. M. *Acc. Chem. Res.* **2001**, *34*, 981.
- (21) (a) Walton, J. C. *J. Chem. Soc., Perkin Trans. 2* **1989**, 173. (b) Costentin, C.; Savéant, J.-M. *J. Phys. Chem.* **2005**, *109*, 4125.
- (18) (a) Bernasconi, C. F.; Ragains, M. L. *J. Am. Chem. Soc.* **2001**, *123*, 11850. (b) Bernasconi, C. F.; Ragains, M. L.; Bhattacharya, S. *J. Am. Chem. Soc.* **2003**, *125*, 12328.
- (19) Fringuelli, F.; Marino, G.; Taticchi, A. *J. Chem. Soc., Perkin Trans. 2* **1974**, 322.
- (20) Bird, C. W. *Tetrahedron* **1985**, *41*, 1409; **1987**, *43*, 4725.

the acidities of $5\text{H}^+-\text{X}$ reflect this order: $\text{p}K_{\text{a}}(5\text{H}^+-\text{O}) = 5.78$,^{18b} $\text{p}K_{\text{a}}(5\text{H}^+-\text{Se}) = 4.18$,^{18a} and $\text{p}K_{\text{a}}(5\text{H}^+-\text{S}) = 2.51$.^{18b}

Inasmuch as aromaticity is related to resonance, a reasonable expectation was that the development of aromaticity at the transition state should also lag behind proton transfer and hence the intrinsic rate constants should be lowest (intrinsic barrier highest) for the most aromatic and highest (intrinsic barrier lowest) for the least aromatic system, i.e., $k_{\text{o}}(\text{O}) > k_{\text{o}}(\text{Se}) > k_{\text{o}}(\text{S})$ or $(\Delta G_{\text{o}}^{\ddagger}(\text{O}) < \Delta G_{\text{o}}^{\ddagger}(\text{Se}) < \Delta G_{\text{o}}^{\ddagger}(\text{S}))$. However, the opposite trend was observed: $k_{\text{o}}(\text{O}) < k_{\text{o}}(\text{Se}) < k_{\text{o}}(\text{S})$ or $(\Delta G_{\text{o}}^{\ddagger}(\text{O}) > \Delta G_{\text{o}}^{\ddagger}(\text{Se}) > \Delta G_{\text{o}}^{\ddagger}(\text{S}))$.^{18b} This is puzzling because, unless the observed trend is caused by some other factors not related to aromaticity, the PNS^{1a-c} implies that development of aromatic stabilization at the transition state has made more progress than proton transfer. Preliminary ab initio calculations on the gas-phase proton transfers from benzenium ion to benzene and from cyclopentadiene to its conjugate anion have led to a similar conclusion,²² i.e., aromatic stabilization at the transition state of the respective identity reactions is more than 50% of that of benzene and cyclopentadienyl anion, respectively.

These results raise the obvious question as to whether they are representative of a general phenomenon or an artifact of the specific systems studied. Hence, it is imperative to examine additional systems for which the dependence of intrinsic rate constants on the degree of aromaticity of the product can be determined. In this paper, we report a kinetic investigation of the reversible deprotonation of benzo[*b*]-2,3-dihydrofuran-2-one (**6H-O**) and benzo[*b*]-2,3-dihydrothiophene-2-one (**6H-S**) by a series of primary aliphatic and secondary alicyclic amines and carboxylate ions (eq 6); the reaction leads to the formation of enolate ions that represent a benzofuran (**6⁻-O**) and a benzothiophene (**6⁻-S**) derivative, respectively. If this system

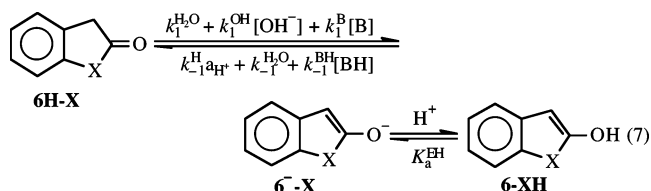


behaves like that in eq 5 one expects $k_{\text{o}}(\text{S}) > k_{\text{o}}(\text{O})$. On the other hand, if the usual pattern observed for common resonance effects is followed, the result should be $k_{\text{o}}(\text{S}) < k_{\text{o}}(\text{O})$.

A more limited investigation of the deprotonation of **6H-O** and **6H-S** involving mainly OH^- and water as the base has already been reported by Kresge and Meng,²³ but their results are not as well suited for the determination of reliable intrinsic rate constants.

Results

General Features. The reactions of **6H-X** in the presence of amine or carboxylate buffers can be described by eq 7 with **6-XH** being the enol form of **6H-X** in rapid equilibrium with the enolate ion and B the buffer base. All kinetic experiments and $\text{p}K_{\text{a}}$ determinations were conducted in water at 25 °C and an ionic strength of 0.1 M (KCl). The $\text{p}K_{\text{a}}^{\text{KH}}$ values of both **6H-O** and **6H-S** were determined kinetically. For **6H-S** the



$\text{p}K_{\text{a}}^{\text{KH}}$ was also obtained spectrophotometrically; for **6H-O** rapid hydrolysis in basic solution made a spectrophotometric determination less desirable. The kinetic experiments were run under pseudo-first-order conditions with the substrate as the minor component. The observed pseudo-first-order rate constants for equilibrium approach are given by eq 8. Most rates were in the stopped-flow time range.

$$k_{\text{obsd}} = k_1^{\text{H}_2\text{O}} + k_1^{\text{OH}^-}[\text{OH}^-] + k_1^{\text{B}}[\text{B}] + (k_{-1}^{\text{H}}a_{\text{H}^+} + k_{-1}^{\text{H}_2\text{O}} + k_{-1}^{\text{BH}^+}[\text{BH}^+]) \frac{K_{\text{a}}^{\text{EH}}}{K_{\text{a}}^{\text{EH}} + a_{\text{H}^+}} \quad (8)$$

Depending on the pH the reactions were conducted in the “forward direction” ($\text{pH} > \text{p}K_{\text{a}}^{\text{KH}}$) or the “reverse direction” ($\text{pH} < \text{p}K_{\text{a}}^{\text{KH}}$). In the latter case, the ketone was first incubated in a 0.025 M KOH solution in order to convert it into its enolate ion; this was followed by mixing the enolate ion with the appropriate buffer in the stopped-flow apparatus. In the case of **6H-O** rapid hydrolysis of the ketone in basic solution required the use of a double mixing stopped-flow apparatus as described in the Experimental Section.

Benzo[*b*]-2,3-dihydrofuran-2-one (6H-O). A. Kinetics in KOH Solution. In KOH solution eq 8 simplifies to eq 9.

$$k_{\text{obsd}} = k_1^{\text{H}_2\text{O}} + k_1^{\text{OH}^-}[\text{OH}^-] \quad (9)$$

A plot of k_{obsd} vs $[\text{KOH}]$ is shown in Figure 1. It yields $(2.44 \pm 0.05) \times 10^3 \text{ M}^{-1} \text{ s}^{-1}$ and $k_{-1}^{\text{H}_2\text{O}} = 20.2 \pm 2.5 \text{ s}^{-1}$ from which $K_{\text{a}}^{\text{KH}} = (k_1^{\text{OH}^-}/k_{-1}^{\text{H}_2\text{O}})K_{\text{w}}^{24} = (1.91 \pm 0.31) \times 10^{-12} \text{ M}^{-1}$ or $\text{p}K_{\text{a}}^{\text{KH}} = 11.72 \pm 0.05$ is obtained. Our results are in reasonably good agreement with those reported by Kresge and Meng²³ in NaOH solution: $k_1^{\text{OH}^-} = 2.24 \times 10^3 \text{ M}^{-1} \text{ s}^{-1}$, $k_{-1}^{\text{H}_2\text{O}} = 26.5 \text{ s}^{-1}$, and $\text{p}K_{\text{a}}^{\text{KH}} = 11.87$.

B. Kinetics in Amine Buffers. Because of the high $\text{p}K_{\text{a}}^{\text{KH}}$ of **6H-O** the equilibrium favors ketone over the enolate ion in most amine buffers. Hence, the kinetic runs were conducted in the “reverse direction”, i.e., by first generating the enolate ion in a dilute KOH solution (typically 0.025 M) followed by mixing with the appropriate amine buffer in the stopped-flow apparatus.

The reactions with the following amines were examined: *n*-butylamine, 2-methoxyethylamine, glycylamide, 2-chloroethylamine, piperidine, piperazine, 1-(2-hydroxyethyl)piperazine (HEPA), and morpholine. The kinetic experiments were performed at five to seven amine concentrations at constant pH.

(1) *n*-Butylamine. With *n*-butylamine the reactions were run at four different pH values between pH 10.48 and 11.35. Plots of k_{obsd} vs free amine are shown in Figure S1 of the Supporting Information.²⁵ The slopes of these plots are given by eq 10.

(24) $\text{p}K_{\text{w}} = 13.8$ at 25 °C and $\mu = 0.1 \text{ M}$.²³

(25) See paragraph concerning Supporting Information at the end of this paper.

(21) Minkin, V. I.; Glukhovtsev, M. N.; Simkin, B. Y. *Aromaticity and Antiaromaticity*; Wiley & Sons: New York, 1994; p 217.

(22) (a) Bernasconi, C. F.; Ragains, M. L.; Wenzel, P. J. to be published.

(b) Bernasconi, C. F. *J. Phys. Org. Chem.* **2004**, *17*, 951.

(23) Kresge, A. J.; Meng, Q. *J. Am. Chem. Soc.* **2002**, *124*, 9189.

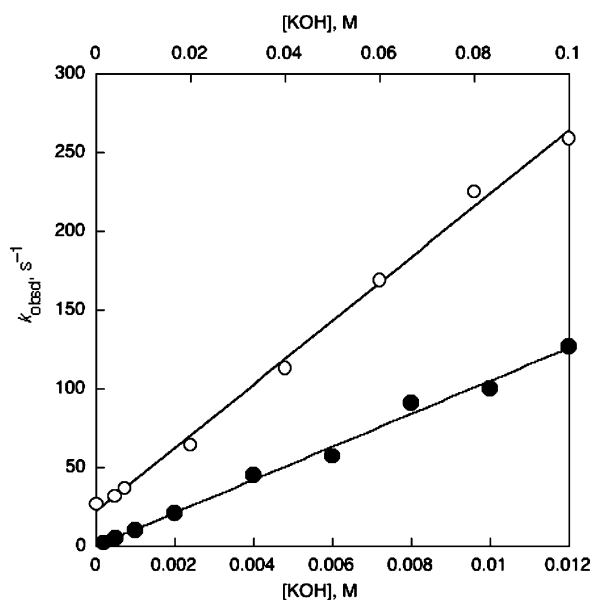


FIGURE 1. Reactions of KOH with **6H-O** (○, top KOH axis) and **6H-S** (●, bottom KOH axis).

From a plot of slope vs a_{H^+}

$$\text{slope} = k_1^{\text{B}} + k_{-1}^{\text{BH}} \frac{a_{\text{H}^+}}{K_{\text{a}}^{\text{BH}}} = k_1^{\text{B}} \left(1 + \frac{a_{\text{H}^+}}{K_{\text{a}}^{\text{KH}}} \right) \quad (10)$$

according to eq 10 (not shown) one obtains $k_1^{\text{B}} = (3.25 \pm 0.75) \times 10^2 \text{ M}^{-1} \text{ s}^{-1}$ and $\text{p}K_{\text{a}}^{\text{KH}} = 11.65 \pm 0.08$. The $\text{p}K_{\text{a}}^{\text{KH}}$ value obtained from these experiments is in good agreement with the one determined in KOH solutions (11.72 ± 0.05) and demonstrates good internal consistency of our data. We shall adopt the average between these two values (11.68) as the $\text{p}K_{\text{a}}^{\text{KH}}$ for **6H-O**. From $k_1^{\text{B}}/k_{-1}^{\text{BH}} = K_{\text{a}}^{\text{KH}}/K_{\text{a}}^{\text{BH}}$ and using $\text{p}K_{\text{a}}^{\text{BH}} = 10.78$ we obtain $k_{-1}^{\text{BH}} = (2.58 \pm 0.65) \times 10^3 \text{ M}^{-1} \text{ s}^{-1}$.

(2) **Glycinamide**. For this amine runs were performed at six different pH values between 7.56 and 8.87. Plots of k_{obsd} vs free amine concentration are shown in Figure S2 (Supporting Information).²⁵ In this pH range, the enol/enolate ion equilibrium is no longer negligible, and hence, the slopes are given by eq 11. A plot of the slopes vs a_{H^+} according to eq 11 is shown in Figure 2. Since K_{a}^{KH} is known, there are only two unknown parameters (k_1^{B} and K_{a}^{EH}) which were obtained by nonlinear least squares curve fitting: $k_1^{\text{B}} = 8.80 \pm 0.20 \text{ M}^{-1} \text{ s}^{-1}$ and $\text{p}K_{\text{a}}^{\text{EH}} = 8.10 \pm 0.04$; k_{-1}^{BH} was calculated as $k_1^{\text{B}} K_{\text{a}}^{\text{BH}}/K_{\text{a}}^{\text{KH}}$ as for the *n*-butylamine reaction.

$$\text{slope} = k_1^{\text{B}} + k_{-1}^{\text{BH}} \frac{a_{\text{H}^+}}{K_{\text{a}}^{\text{BH}}} \frac{K_{\text{a}}^{\text{EH}}}{K_{\text{a}}^{\text{EH}} + a_{\text{H}^+}} = k_1^{\text{B}} \left(1 + \frac{a_{\text{H}^+}}{K_{\text{a}}^{\text{KH}}} \frac{K_{\text{a}}^{\text{EH}}}{K_{\text{a}}^{\text{EH}} + a_{\text{H}^+}} \right) \quad (11)$$

(3) **2-Methoxyethylamine, 2-Chloroethylamine, Piperidine, Piperazine, HEPA, and Morpholine**. With these amines kinetic runs were performed at 1:1 buffer ratios only, corresponding to $\text{pH} = \text{p}K_{\text{a}}^{\text{BH}}$. Equations 10 or 11 were used to obtain k_1^{B} as the only unknown, while k_{-1}^{BH} was calculated as before.

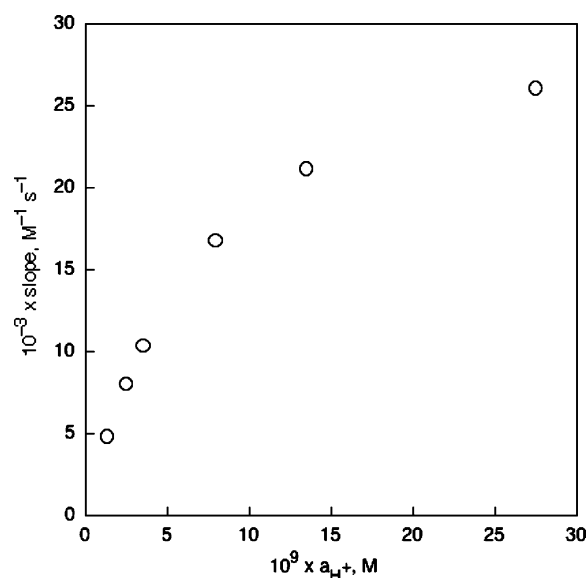


FIGURE 2. Slopes according to eq 11 for the reaction of **6H-O** with glycinamide.

C. Kinetics in Carboxylate Buffers. Attempts at measuring rates with carboxylate buffers were unsuccessful because the reactions were beyond the time range of the stopped-flow method.

Benzo[*b*]-2,3-dihydrothiophene-2-one (6H-S). A. Spectrophotometric $\text{p}K_{\text{a}}^{\text{KH}}$ Determination. The $\text{p}K_{\text{a}}^{\text{KH}}$ determination was based on eq 12 where A_{E} is the absorbance of the enolate ion ($\text{pH} \gg \text{p}K_{\text{a}}^{\text{KH}}$), A_{KH} the absorbance of the ketone ($\text{pH} \ll \text{p}K_{\text{a}}^{\text{KH}}$), and A the absorbance at $\text{pH} \sim \text{p}K_{\text{a}}^{\text{KH}}$. A plot of pH vs $\log(A_{\text{E}} - A)/(A - A_{\text{KH}})$ is shown in Figure S3 (Supporting Information).²⁵ Its slope of 1.03 ± 0.02 is close to the expected value, and the intercept yields $\text{p}K_{\text{a}}^{\text{KH}} = 8.84 \pm 0.03$.

$$\text{pH} = \text{p}K_{\text{a}}^{\text{KH}} + \log \frac{A_{\text{E}} - A}{A - A_{\text{KH}}} \quad (12)$$

B. Kinetics in KOH Solutions. A plot of k_{obsd} vs [KOH] (Figure 1) yields $k_1^{\text{OH}} = (1.05 \pm 0.03) \times 10^4 \text{ M}^{-1} \text{ s}^{-1}$ and $k_{-1}^{\text{O}} = 0.113 \pm 0.015 \text{ s}^{-1}$ (eq 9) from which $K_{\text{a}}^{\text{KH}} = (k_1^{\text{OH}}/k_{-1}^{\text{O}})K_{\text{w}}^{24} = (1.47 \pm 0.28) \times 10^{-9}$ or $\text{p}K_{\text{a}}^{\text{KH}} = 8.83 \pm 0.06$. The close agreement of this $\text{p}K_{\text{a}}^{\text{KH}}$ value with that determined spectrophotometrically is fortuitous because the intercept (k_{-1}^{O}) is so small that its potential uncertainty is probably larger than its standard deviation.

B. Kinetics in Amine Buffers. Since the $\text{p}K_{\text{a}}^{\text{KH}}$ of **6H-S** (8.84) is much lower than that of **6H-O** (11.68) all kinetic runs could be conducted in the “forward direction”, i.e., by mixing a ketone solution with the appropriate amine buffer in the stopped-flow spectrophotometer. The same amines were used as for the reactions of **6H-O**.

(1) **2-Chloroethylamine**. With 2-chloroethylamine, kinetic runs were performed at six different pH values between pH 7.90 and 9.15. Plots of k_{obsd} vs free amine concentration are shown in Figure S4 (Supporting Information).²⁵ The slopes are given by eq 10; a plot of slope vs a_{H^+} (Figure S5, Supporting Information²⁵) yielded $k_1^{\text{B}} = (1.96 \pm 0.02) \times 10^2 \text{ M}^{-1} \text{ s}^{-1}$ and $\text{p}K_{\text{a}}^{\text{KH}} = 8.80 \pm 0.03$ in excellent agreement with the spectrophotometric value of 8.84. We shall adopt the average of these two values, 8.82, as the actual $\text{p}K_{\text{a}}^{\text{KH}}$.

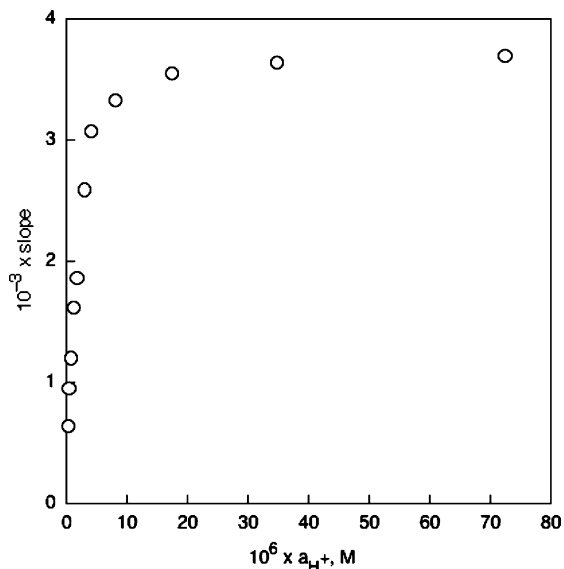


FIGURE 3. Slopes according to eq 11 for the reaction of **6H-S** with acetate ion.

(2) *n*-Butylamine, 2-Methoxyethylamine, Glycinamide, Aminoacetonitrile, Piperidine, Piperazine, HEPA, and Morpholine. With these amines, the reactions were run in 1:1 buffers ($\text{pH} = \text{p}K_{\text{a}}^{\text{BH}}$). Equation 10 was used to obtain k_1^{B} , while k_{-1}^{BH} was calculated as $k_1^{\text{B}}K_{\text{a}}^{\text{BH}}/K_{\text{a}}^{\text{KH}}$ except for the aminoacetonitrile reaction where eq 11 was used.

C. Kinetics in Carboxylate Buffers. All kinetic runs were conducted in the “reverse direction” as described for the reactions of **6H-O**.

(1) **Acetic Acid.** With acetate buffers, runs were performed at nine pH values between 4.76 and 6.35. Plots of k_{obsd} vs acetate ion concentration are shown in Figure S6 (Supporting Information).²⁵ Since in this pH range the enol/enolate equilibrium becomes significant, the slopes are given by eq 11. A plot of the slopes vs a_{H^+} is shown in Figure 3. Nonlinear least-squares analysis yields $k_1^{\text{B}} = 3.85 \pm 0.25$ and $\text{p}K_{\text{a}}^{\text{EH}} = 5.82 \pm 0.04$.

(2) **Methoxyacetic, Chloroacetic, and Dichloroacetic Acid.** With these acids runs were performed at 1:1 buffer ratios only. Equation 11 was used to obtain k_1^{B} as the only unknown.

Discussion

The various rate constants and $\text{p}K_{\text{a}}$ values determined in this study along with parameters reported by Kresge and Meng²³ are summarized in Tables 1 and 2.

General Observations and Comparisons with Previous Work. There is some overlap between our work and that reported by Kresge and Meng,²³ in particular with respect to the $\text{p}K_{\text{a}}^{\text{KH}}$ and $\text{p}K_{\text{a}}^{\text{EH}}$ values, and the rate constants for the reversible deprotonation of the two substrates by OH^- (k_1^{OH} and $k_{-1}^{\text{H}_2\text{O}}$) are summarized in Table 1. The agreement between the results from the two laboratories ranges from excellent ($\text{p}K_{\text{a}}^{\text{KH}}$ of **6H-S**, k_1^{OH} for **6H-O**, and **6H-S**, $\Delta G_{\text{o}}^{\ddagger}$ for **6H-O** and **6H-S**) to good ($\text{p}K_{\text{a}}^{\text{KH}}$ of **6H-O**, $k_{-1}^{\text{H}_2\text{O}}$ for **6H-O** and **6H-S**) to fair ($\text{p}K_{\text{a}}^{\text{EH}}$ for **6H-S**). The reason for the relatively large discrepancy in the $\text{p}K_{\text{a}}^{\text{EH}}$ values for **6H-S** between the two laboratories (0.6 pK units) is not clear except that the methods for obtaining the $\text{p}K_{\text{a}}^{\text{EH}}$ values were different. Ours was based

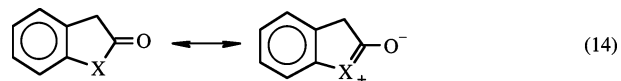
on rate constants for acetate buffer catalysis (Figures S6 (Supporting Information) and 3, eq 11); i.e., we made use of the pH dependence of slopes of buffer plots. Kresge and Meng relied on a rate–pH profile which was constructed from zero buffer concentration intercepts. When buffer catalysis is strong, as was the case in our reactions (see Figure S6, Supporting Information), slopes generally can be determined more reliably than intercepts and this could be the reason for the observed discrepancy.

The kinetic experiments for the reactions of **6H-O** with the amines and of **6H-S** with the carboxylate ions had to be conducted in the reverse direction, i.e., by generating the respective enolate ion in dilute KOH solution prior to mixing with the buffer. In the case of **6H-O** the problem of its rapid hydrolysis in basic solution²⁶ was solved by using a dual-mixing stopped-flow apparatus. This allowed us to determine proton-transfer intrinsic rate constants with amines for both **6H-S** and **6H-O**, which is the major focus of our study.

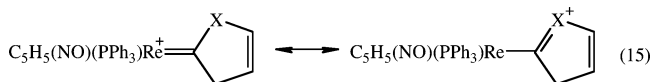
Regarding the acidities of **6H-O** and **6H-S**, from the difference between $\text{p}K_{\text{a}}^{\text{KH}}$ and $\text{p}K_{\text{a}}^{\text{EH}}$ values (eq 13) one can calculate the $\text{p}K_{\text{E}}$ for the enolization equilibrium constants; they are quite similar for **6H-O** (3.58) and **6H-S** (3.00).

$$\text{p}K_{\text{E}} = \text{p}K_{\text{a}}^{\text{KH}} - \text{p}K_{\text{a}}^{\text{EH}} \quad (13)$$

6H-S ($\text{p}K_{\text{a}}^{\text{KH}} = 8.82$) is significantly more acidic than **6H-O** ($\text{p}K_{\text{a}}^{\text{KH}} = 11.68$). Kresge and Meng²³ have attributed the higher acidity of **6H-S** to the greater aromatic stabilization of the thiophene ring in **6-S** compared to that of the furan ring in **6-O**.^{19–21} A contributing factor to the acidity difference may be the stronger π -donor effect of the ring oxygen in **6H-O** compared to that of the ring sulfur in **6H-S**; the greater stabilization of **6H-O** should reduce its acidity more than that of **6H-S**.



By way of comparison, the $\text{p}K_{\text{a}}$ difference between **5H⁺-O** ($\text{p}K_{\text{a}} = 5.78$) and **5H⁺-S** ($\text{p}K_{\text{a}} = 2.51$) is 3.27,¹⁸ which is similar to that between **6H-O** and **6H-S**. Here, too, the difference in the π -donor effect may contribute to the difference in acidities.



Brønsted Plots and Intrinsic Rate Constants. Brønsted plots for the reactions of **6H-O** are shown in Figure 4, those for **6H-O** in Figure 5. The Brønsted α and β values, $\log k_{\text{o}}$ for the intrinsic rate constants determined from the point where the lines for k_1^{B} and k_{-1}^{BH} intersect, and $\Delta G_{\text{o}}^{\ddagger}$ calculated from k_{o} by means of the Eyring equation are summarized in Table 3, along with the corresponding parameters for deprotonation of the rhenium Fischer carbene complexes of eq 5.¹³ The following points are noteworthy.

(1) The Brønsted α and β values are within the typical range observed for proton transfers to and from carbon,^{27,28} as was also reported for the reactions of **5H⁺-O** and **5H⁺-S**.¹⁸

(26) Kresge, A. J. Personal communication.

(27) (a) Bell, R. P. *The Proton in Chemistry*, 2nd ed.; Cornell University Press: Ithaca, 1973; Chapter 10. (b) Kresge, A. J. In *Proton-Transfer Reactions*; Caldin, E. F., Gold V., Eds.; Wiley: New York, 1975; p 179.

TABLE 1. Rate Constants, Intrinsic Barriers, and pK_a Values for the Reversible Deprotonation of **6H-O** and **6H-S** by OH^- in Water at 25 °C, $\mu = 0.1$ M (KCl)

parameter	6H-O		6H-S	
	this work	Kresge et al. ^a	this work	Kresge et al. ^a
$k_1^{OH}, M^{-1} s^{-1}$	$(2.44 \pm 0.05) \times 10^3$	2.24×10^3	$(1.05 \pm 0.03) \times 10^4$	9.55×10^3
$k_{-1}^{H_2O}, s^{-1}$	20.2 ± 2.5	26.5	0.113 ± 0.015	0.0794
ΔG_o^\ddagger , kcal/mol	14.1 ^b	14.1 ^{b,c}	15.1 ^b	15.3 ^b
pK_a^{KH}	11.68 ± 0.04^d	11.87	8.82 ± 0.03	8.85
pK_a^{EH}	8.10 ± 0.04		5.82 ± 0.04	5.23
$pK_E = pK_a^{KH} - pK_a^{EH}$	3.58 ± 0.07		3.00 ± 0.07	3.62

^a Reference 23. ^b Calculated based on eq 16. ^c This value was not reported in ref 23 but was calculated on the basis of Kresge and Meng's k_1^{OH} and $k_{-1}^{H_2O}$ values. ^d Average of pK_a^{KH} determined from kinetic experiments with KOH and with *n*-BuNH₂.

TABLE 2. Rate Constants for the Reversible Deprotonation of **6H-O** and **6H-S** by Amines and Carboxylate Ions and pK_a Values in Water at 25 °C, $\mu = 0.1$ M (KCl)

B	pK_a^{BH}	$k_1^B, M^{-1} s^{-1}$	$k_{-1}^{BH}, M^{-1} s^{-1}$
6H-O ($pK_a^{KH} = 11.68 \pm 0.04$; $pK_a^{EH} = 8.10 \pm 0.03$)			
<i>n</i> -BuNH ₂	10.78	$(3.25 \pm 0.75) \times 10^2$	$(2.58 \pm 0.65) \times 10^3$
MeOCH ₂ CH ₂ NH ₂	9.61	$(7.25 \pm 0.03) \times 10^1$	$(8.62 \pm 0.04) \times 10^3$
ClCH ₂ CH ₂ NH ₂	8.77	$(2.90 \pm 0.02) \times 10^1$	$(2.35 \pm 0.02) \times 10^4$
H ₂ NCOCH ₂ NH ₂	8.10	8.80 ± 0.20	$(3.32 \pm 0.10) \times 10^4$
piperidine	11.26	$(1.32 \pm 0.02) \times 10^3$	$(3.50 \pm 0.07) \times 10^3$
piperazine	10.00	$(2.98 \pm 0.06) \times 10^2$	$(1.43 \pm 0.04) \times 10^4$
HEPA ^a	9.44	$(1.44 \pm 0.01) \times 10^2$	$(2.50 \pm 0.02) \times 10^4$
morpholine	8.95	$(5.37 \pm 0.04) \times 10^1$	$(2.88 \pm 0.02) \times 10^4$
6H-S ($pK_a^{KH} = 8.82 \pm 0.02$; $pK_a^{EH} = 5.82$)			
<i>n</i> -BuNH ₂	10.78	$(1.03 \pm 0.01) \times 10^3$	$(1.13 \pm 0.11) \times 10^1$
MeOCH ₂ CH ₂ NH ₂	9.61	$(4.51 \pm 0.05) \times 10^2$	$(7.39 \pm 0.70) \times 10^1$
ClCH ₂ CH ₂ NH ₂	8.77	$(1.96 \pm 0.02) \times 10^2$	$(2.19 \pm 0.02) \times 10^2$
H ₂ NCOCH ₂ NH ₂	8.10	$(1.31 \pm 0.01) \times 10^2$	$(6.84 \pm 0.02) \times 10^2$
NCCH ₂ NH ₂	5.45	$(5.78 \pm 0.23) \times 10^0$	$(1.36 \pm 0.07) \times 10^4$
piperidine	11.26	$(1.27 \pm 0.08) \times 10^4$	$(4.66 \pm 0.02) \times 10^1$
piperazine	10.00	$(4.59 \pm 0.01) \times 10^3$	$(3.03 \pm 0.03) \times 10^2$
HEPA ^a	9.44	$(3.10 \pm 0.07) \times 10^3$	$(7.43 \pm 0.07) \times 10^2$
morpholine	8.95	$(1.36 \pm 0.03) \times 10^3$	$(1.01 \pm 0.10) \times 10^3$
CH ₃ CO ₂ ⁻	4.76	3.85 ± 0.25	$(4.42 \pm 0.30) \times 10^4$
MeOCH ₂ CO ₂ ⁻	3.54	1.41 ± 0.03	$(2.69 \pm 0.12) \times 10^5$
ClCH ₂ CO ₂ ⁻	2.86	0.71 ± 0.03	$(6.46 \pm 0.27) \times 10^5$
Cl ₂ CHCO ₂ ⁻	1.29	0.062 ± 0.002	$(2.10 \pm 0.09) \times 10^6$

^a 1-(2-Hydroxyethyl)piperazine.

(2) For each carbon acid $\log k_o$ for the reactions with the secondary amines is larger than for the reactions with the primary amines. This reflects a generally observed reactivity pattern in proton transfers at carbon; it is the result of differences in the solvation energies of the respective protonated amines and the fact that at the transition state solvation of the incipient protonated amines lags behind the proton transfer.^{27a,29}

(3) The intrinsic rate constants (intrinsic barriers) for the deprotonation of **6H-O** appear to be higher (lower) than for the deprotonation of **6H-S**. For the reaction with primary amines $\log k_o(O)/k_o(S) = \Delta \log k_o = 0.65 \pm 0.12$ ($\Delta \Delta G_o^\ddagger = -0.94 \pm 0.16$) is definitely positive (negative) while for the reaction with the secondary amines $\log k_o(O)/k_o(S) = \Delta \log k_o = 0.24 \pm 0.16$ ($\Delta \Delta G_o^\ddagger = -0.26 \pm 0.21$) suggests that the intrinsic rate constant (intrinsic barrier) for **6H-O** is either marginally higher (lower) or comparable to that for **6H-S**.

These results contrast strongly with those for the carbene complexes where with both types of amines $\log k_o$ for the furan

(28) (a) Bernasconi, C. F.; Paschalis, P. *J. Am. Chem. Soc.* **1986**, *108*, 2969. (b) Bernasconi, C. F.; Terrier, F. *J. Am. Chem. Soc.* **1987**, *109*, 7115. (c) Bernasconi, C. F.; Kliner, D. A. V.; Mullin, A. S.; Ni, X. *J. Org. Chem.* **1988**, *53*, 3342.

(29) Jencks, W. P. *Catalysis in Chemistry and Enzymology*; McGraw-Hill: New York, 1969; p 178.

derivative is lower than for the thiophene derivative ($\log k_o(O)/k_o(S) = \Delta \log k_o = -1.10 \pm 0.56$ for the primary amines, $\Delta \log k_o = -1.51 \pm 0.89$ for the secondary amines). In other words, our results suggest that the reactions of **6H-O** and **6H-S** follow the pattern typical for reactions that lead to products stabilized by resonance/delocalization.

For the deprotonation of **6H-O** and **6H-S** by OH^- one may also calculate approximate intrinsic barriers by applying the Marcus³ relationship (eq 16). Again we see that the intrinsic barrier is lower for the reaction of **6H-O** than for the reaction of **6H-S**.

$$\Delta G^\ddagger = \Delta G_o^\ddagger \left(1 + \frac{\Delta G_o^\circ}{4\Delta G_o^\ddagger} \right)^2 \quad (16)$$

Why Does 6H-X Behave Differently from 5H⁺-X? Without a larger database that would allow one to uncover broader trends it is difficult to provide an unambiguous explanation as to why the two systems behave differently with respect to the effect of the aromaticity on the intrinsic barriers. It is not even clear whether aromaticity is the key factor. However, it is reasonable to assume that a primary source for the different behavior of the two systems is a difference in the influence of the heteroatoms in the two systems beyond their effect on aromaticity. The heteroatom in other carbene complexes is known to substantially influence intrinsic barriers of proton transfer by a number of different interaction mechanisms. They have been discussed in detail in the context of comparisons between the deprotonation of **7H-O** and **7H-S**^{5b} (data included in Table 3).



The main conclusions from these comparisons can be summarized as follows. (1) The stronger electron-withdrawing inductive effect of the MeO compared to the MeS group enhances k_o for **7H-O** relative to that of **7H-S**. This is because, at the transition state, the incipient negative charge is closer to the heteroatom than it is in the product anion which means the transition-state stabilization by the inductive effect is disproportionately strong relative to the stabilization of the anion. (2) The larger size of the MeS group leads to enhanced steric crowding at the transition state which lowers k_o for **7H-S** relative to k_o for **7H-O**. Both the electronic and steric factors are believed to contribute to the fact that $k_o(O)/k_o(S) > 1$. (3) The π -donor effect of the MeO and MeS groups may also affect the intrinsic rate constants but so far it has remained unclear whether it

TABLE 3. Brønsted α and β Values, $\log k_o$ Values for the Intrinsic Rate Constants, and Intrinsic Barriers (ΔG_o^\ddagger)

	$\beta = (d \log k_1^B) / (d \log K_a^{BH})$	$\alpha = (d \log k_{-1}^{BH}) / (d \log K_a^{BH})$	$\log k_o$	$\log(k_o(O)/k_o(S)) = \Delta \log k_o$	ΔG_o^\ddagger , kcal/mol	$\Delta \Delta G_o^\ddagger$, kcal/mol
6H-O^a						
primary amines	0.57 ± 0.03	0.43 ± 0.03	2.77 ± 0.03		13.6 ± 0.1	
secondary amines	0.58 ± 0.05	0.42 ± 0.05	3.23 ± 0.08		13.0 ± 0.1	
6H-S^a						
primary amines	0.43 ± 0.03	0.57 ± 0.03	2.08 ± 0.05	0.69 ± 0.08	14.5 ± 0.1	-0.94 ± 0.16
secondary amines	0.40 ± 0.05	0.60 ± 0.05	2.99 ± 0.08	0.24 ± 0.16	13.3 ± 0.1	-0.33 ± 0.21
carboxylate ions	0.52 ± 0.06	0.48 ± 0.06	2.67 ± 0.34		13.7 ± 0.5	
5H⁺-O^b						
primary amines	0.53 ± 0.06	0.47 ± 0.06	-0.83 ± 0.22		18.5 ± 0.3	
secondary amines	0.65 ± 0.08	0.35 ± 0.08	-0.46 ± 0.35		17.9 ± 0.5	
5H⁺-S^b						
primary amines	0.42 ± 0.05	0.58 ± 0.05	0.27 ± 0.34	-1.10 ± 0.56	17.0 ± 0.5	1.50 ± 0.76
secondary amines	0.40 ± 0.07	0.60 ± 0.07	1.05 ± 0.54	-1.51 ± 0.89	15.9 ± 0.7	2.05 ± 1.21
7H-O^c						
primary amines	0.61 ± 0.06	0.39 ± 0.06	3.04 ± 0.17		13.2 ± 0.2	
secondary amines	0.62 ± 0.03	0.38 ± 0.03	3.70 ± 0.70		12.3 ± 0.1	
7H-S^c						
primary amines	0.48 ± 0.04	0.52 ± 0.04	2.09 ± 0.08	0.95 ± 0.25	14.5 ± 0.1	-1.29 ± 0.34
secondary amines	0.48 ± 0.06	0.55 ± 0.06	2.61 ± 0.10	1.09 ± 0.17	13.8 ± 0.1	-1.48 ± 0.23

^a In water at 25 °C, $\mu = 0.1$ M (KCl), this work. ^b In 50% MeCN–50% water (v/v) at 25 °C, $\mu = 0.1$ M (KCl), ref 18. ^c In 50% MeCN–50% water (v/v) at 25 °C, $\mu = 0.1$ M, ref 5b. ^d $\Delta \Delta G_o^\ddagger = \Delta G_o^\ddagger(O) - \Delta G_o^\ddagger(S)$.

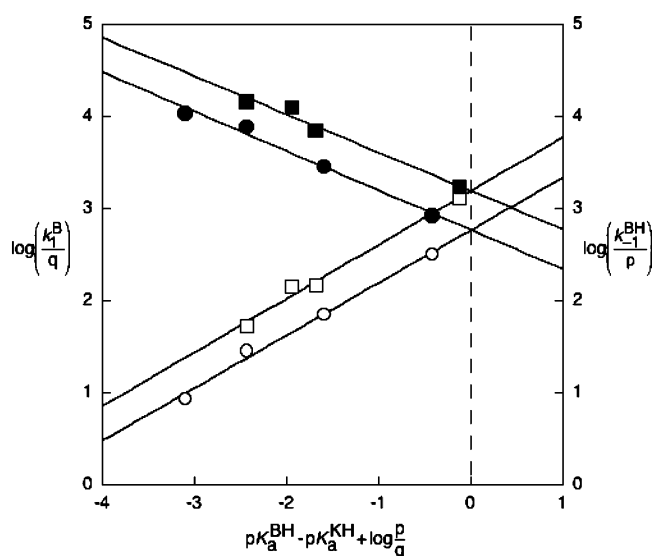
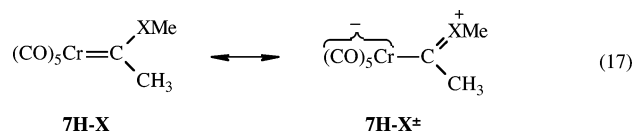


FIGURE 4. Brønsted plots for the reactions of **6H-O** with amine buffers: open symbols, k_1^B ; filled symbols, k_{-1}^{BH} ; \bullet , \circ , primary aliphatic amines; \square , \blacksquare , secondary alicyclic amines. The dashed line goes through the points where the $\log(k_1^B/q)$ and $\log(k_{-1}^{BH}/p)$ lines intersect, which corresponds to $\log k_o$.

enhances or lowers k_o because there are two potentially opposing factors. The first factor (“Type I π -donor effect”) is the loss of the resonance stabilization of **7H-X[±]** (eq 17) which is expected



to follow the general rule for resonance effects, i.e., its loss is ahead of proton transfer at the transition state which lowers k_o . Since the MeO group is a stronger π -donor than the MeS group²⁹

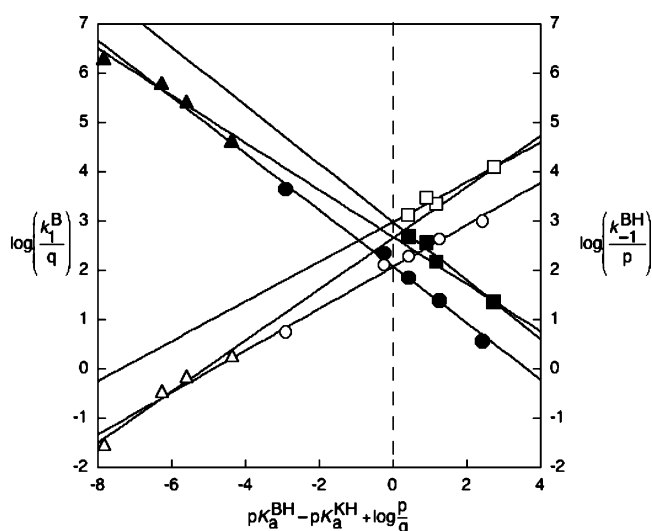


FIGURE 5. Brønsted plots for the reactions of **6H-S** with amine and carboxylate buffers: open symbols, k_1^B ; filled symbols, k_{-1}^{BH} ; \circ , \bullet , primary aliphatic amines; \square , \blacksquare , secondary alicyclic amines; \triangle , \blacktriangle , carboxylate ions. The dashed line goes through the points where the $\log(k_1^B/q)$ and $\log(k_{-1}^{BH}/p)$ lines intersect, which corresponds to $\log k_o$.

there is a greater decrease in k_o for **7H-O** than for **7H-S**, and hence, this factor decreases the $k_o(O)/k_o(S)$ ratio. The second factor (“Type II π -donor effect”) is the preorganization of the $(\text{CO})_5\text{Cr}$ group of **7H-X** in **7H[±]-X** toward its electronic configuration in the anion. This preorganization reduces the transition state imbalance and with it its k_o -lowering effect. **7H-O** benefits more than **7H-S** from this effect because of the greater π -donor strength of the MeO; hence, this factor enhances the $k_o(O)/k_o(S)$ ratio.

The various effects of the heteroatoms on $k_o(O)$, $k_o(S)$, and the $k_o(O)/k_o(S)$ ratio discussed above are schematically summarized in Table 4. In the absence of aromaticity effects and unless the π -donor effect related to the loss of reactant resonance (type I) is overriding all other factors, one expects $k_o(O)/k_o(S) > 1$ as observed for the **7H-X** system. Now let us assume

TABLE 4. Effect of Heteroatom on the Intrinsic Rate Constants^a

	$k_o(\text{O})$	$k_o(\text{S})$	$\frac{k_o(\text{O})}{k_o(\text{S})}$
Inductive effect	↑	↑	↑
Steric effect	↓	↓	↑
Type I π -donor effect ^b	↓	↓	↓
Type II π -donor effect ^c	↑	↑	↑
Aromaticity: Hypothesis A ^d	↓	↓	↑
Aromaticity: Hypothesis B ^e	↑	↑	↓

^a Arrows pointing up imply an increase, arrows pointing down imply a decrease. The lengths of the arrows indicate whether the effect is large or small. ^b Loss of resonance stabilization of carbon acid. ^c Preorganization factor. ^d Aromaticity lags behind proton transfer. ^e Aromaticity is ahead of proton transfer.

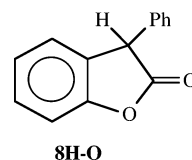
(hypothesis A) that the effect of aromaticity on intrinsic rate constants is qualitatively the same as that of resonance; i.e., it lowers k_o . This would contribute to an increase in the $k_o(\text{O})/k_o(\text{S})$ ratio. Hence, if the inductive, steric and π -donor effects in the **6H-X** system were of similar magnitude as in the **7H-X** system, one would expect the $k_o(\text{O})/k_o(\text{S})$ ratio for the **6H-X** system to be larger than for the **7H-X** system. However, the $k_o(\text{O})/k_o(\text{S})$ ratios are *smaller*: for **6H-X** $\Delta\log k_o = 0.65 \pm 0.12$ with primary amines and $\Delta\log k_o = 0.19 \pm 0.16$ with secondary amines, while for the **7H-X** systems $\Delta\log k_o = 0.95 \pm 0.25$ with primary amines and $\Delta\log k_o = 1.09 \pm 0.17$ for secondary amines. We conclude that either hypothesis A is incorrect or that the magnitudes of the inductive, steric, and π -donor effect of the heteroatoms are quite different in the two systems. Regarding the carbene complex system **5H⁺-X**, based on hypothesis A, the discrepancy between expectation and actual result is even greater since here $k_o(\text{O})/k_o(\text{S}) < 1$ ($\Delta\log k_o = -1.10 \pm 0.56$ with primary amines and $\Delta\log k_o = -1.51 \pm 0.59$ with secondary amines). Reconciliation with hypothesis A would require a strong enhancement in the type I π -donor effect in the **5H⁺-X** system without a corresponding increase in the type II π -donor effect. In view of the cationic nature of **5H⁺-X** where the π -donation leads to *charge delocalization* (eq 15) rather than *charge separation* (eqs 14, 17), such an enhanced π -donor effect cannot be ruled out. The much lower absolute values of k_o for the reactions of **5H⁺-X** (Table 3) compared to those for the reactions of **6H-X** and **7H-X** would be in agreement with such an enhanced type I π -donor effect.

Let us now consider hypothesis B, which assumes that aromaticity increases intrinsic rate constants and should contribute to a decrease in the $k_o(\text{O})/k_o(\text{S})$ ratio. If we again assume that in the **6H-X** and **7H-X** systems the inductive, steric, and π -donor effects are of similar magnitude, the $k_o(\text{O})/k_o(\text{S})$ ratios should be smaller for the **6H-X** systems than for the **7H-X** systems, as observed. The same is true for the **5H⁺-X** systems

where $k_o(\text{O})/k_o(\text{S}) < 1$. The smaller $k_o(\text{O})/k_o(\text{S})$ ratio for the **5H⁺-X** system compared to the **6H-X** system could again be explained by the stronger type I π -donor effect.

In conclusion, hypothesis B appears more satisfactory than hypothesis A, but additional systems will have to be examined in order to put our conclusions on firmer ground. Assuming that hypothesis B holds, we note that our analysis suggests that the k_o -enhancing effect of aromaticity is not as dramatic as the results for the **5H⁺-X** system had suggested; the type I π -donor effect which seems particularly strong in the cationic **5H⁺-X** system makes a major contribution to the small $k_o(\text{O})/k_o(\text{S})$ ratio.

Comparison of 6H-O with the Phenyl-Substituted Analogue. A comparison between **6H-O** and its phenyl-substituted analogue (3-phenylcoumaran-2-one, **8H-O**) is interesting. Heath-



cote et al.³² report a $\text{p}K_a^{\text{KH}} = 8.39$ and $\text{p}K_a^{\text{EH}} < 6.39$ in water; in 50% dioxane–50% water (v/v) $\text{p}K_a^{\text{KH}} = 8.86$, $\text{p}K_a^{\text{EH}} = 6.0$ and $\text{p}K_E = 2.9$. These results indicate a strong enolate ion-stabilizing effect of the phenyl group without significantly changing the $\text{p}K_E$ (Table 1). It was also reported that the $\log k_o$ value for the deprotonation of **8H-O** by a series of aminosulfonic acids in 50% dioxane–50% water (v/v) at 25 °C is 2.60.³² This is somewhat lower than the intrinsic rate constant for the deprotonation of **6H-O** by aliphatic amines ($\log k_o = 2.77$) or secondary alicyclic amines ($\log k_o = 3.23$) in water. In view of the substantial resonance effect of the phenyl group on the stabilization of the enolate ion such a reduction is expected,^{1a-c} but the size of the reduction seems rather small. This must be due to reduced hydrogen-bonding solvation of the enolate ion in 50% dioxane–50% water; i.e., in pure water $\log k_o$ for the deprotonation of **8H-O** is expected to be lower than in the partially organic solvent.³³

Conclusion

The main focus of this paper has been on how the difference in the aromaticity between **6-O** and **6-S** may affect the intrinsic barriers to proton transfer; since **6-O** is a furan and **6-S** a thiophene derivative, the latter is more aromatic as reflected in the higher acidity of **6H-S** compared to **6H-O**. The intrinsic barriers for the deprotonation of **6H-S** by amines and OH^- were found to be somewhat higher than for **6H-O**; this contrasts with the deprotonation of **5H⁺-S** and **5H⁺-O** where the intrinsic barriers for the sulfur derivative are significantly *lower*. Based on the PNS and in the absence of other factors that influence the intrinsic barriers, one would have to conclude that in the **6H-X** system development of aromaticity lags behind proton transfer at the transition state while in the **5H⁺-X** system aromaticity develops ahead of proton transfer. However, a detailed analysis suggests that aromaticity may reduce the

(30) $\sigma_R = -0.43$ and -0.15 for MeO and MeS, respectively.³¹

(31) Hansch, C.; Leo, A.; Taft, R. W. *Chem. Rev.* **1991**, *91*, 165.

(32) Heathcote, D. M.; Atherton, J. H.; De Boes, G. A.; Page, M. I. *J. Chem. Soc., Perkin Trans. 2* **1998**, 541.

(33) Solvation is a product stabilizing factor whose development at the transition state lags behind proton transfer and, hence, according to the PNS,^{1a-1c} lowers the intrinsic rate constant.

intrinsic barriers not only in the $5\text{H}^+\text{-X}$ system but in the 6H-X system as well. The fact that the *observed* intrinsic barriers for 6H-S are somewhat higher than for 6H-O would therefore have to be attributed to a combination of steric, inductive and π -donor effects which overshadow the aromaticity effect. Further work will be needed to reach more definite conclusions.

Experimental Section

Materials. Benzo[*b*]-2,3-dihydrofuran-2-one (6H-O) was commercially available. Benzo[*b*]-2,3-dihydrothiophene-2-one (6H-S) was synthesized as described by Bordwell et al.³⁴ Recrystallization from hexane yielded light yellow prisms, mp 40–43 °C (lit.³⁴ mp 41–44 °C). $^1\text{H NMR } \delta$ (CDCl_3) 3.99 (s, 2H), 7.2–7.4 (m, 4H). The amines in liquid form (*n*-butylamine, methoxyethylamine, piperidine, morpholine, and HEPA) were refluxed over CaH_2 and distilled under argon prior to use. The amines in solid form came as the hydrochloride salt (2-chloroethylamine, glycineamide, aminoacetonitrile, and piperazine) and were used without further purification. The carboxylic acids (99% reagent grade) were used without further purification. KOH (1 M) and HCl solutions were prepared using “Dilut It” from Baker Analytical. Water was taken from a Milli-Q purification system.

(34) Bordwell, F. G.; Fried, H. E. *J. Org. Chem.* **1991**, *56*, 4218.

Kinetics, Spectra, and pH Determinations. All kinetic experiments were performed in water at 25 °C, $\mu = 0.1$ M maintained with KCl. Absorbance changes were monitored at 275 nm (enolate ion of 6H-O) and 286 nm (enolate ion of 6H-S), respectively. Typical substrate concentrations were about 4×10^{-5} M. For the reactions of 6H-O with the amine buffers, 6H-O^- was generated by mixing 6H-O with 0.025 M KOH in a dual mixing stopped-flow spectrophotometer. One to two seconds later this solution was then mixed with the appropriate buffer to induce the desired protonation reaction. For the reactions of 6H-S the stopped-flow apparatus was used in its regular mode. The pH values of the reaction solutions were determined in mock mixing experiments.

Instrumentation. UV–vis spectra were obtained on a diode array spectrophotometer. Kinetic experiments were performed on a stopped-flow apparatus. The pH measurements were carried out with a pH meter equipped with standard glass electrode and a “Sure Flow” reference electrode.

Acknowledgment. This research has been supported by Grant No. CHE-046622 from the National Science Foundation.

Supporting Information Available: Figures S1–S6 (kinetic data). This material is available free of charge via the Internet at <http://pubs.acs.org>.

JO0615899